PROCEEDINGS OF SCIENCE

Studies of cosmic-ray solar modulation with the PAMELA experiment

A. Lenni,[a,b,*] **M. Boezio,**[a,b] **R. Munini,**[a,b] **N. Marcelli,**[a,b] **W. Menn,**[c] **M. S. Potgieter,**[d] **M. D. Ngobeni**[e] **and the PAMELA collaboration**

[a] *INFN, Section of Trieste, I-34127 Trieste, Italy*
[b] *IFPU - Institute of Fundamental Physics of the Universe, I-34151 Trieste, Italy*
[c] *Department of Physics, University of Siegen, D-57068 Siegen, Germany*
[d] *Institute for Experimental and Applied Physics, University of Kiel, D-24118, Kiel, Germany*
[e] *Centre for Space Research, North-West University, 2520, Potchefstroom, South Africa*

E-mail: alex.lenni@ts.infn.it

The launch of the satellite-borne PAMELA instrument on the 15th June 2006 opened a new era of high-precision studies of cosmic rays. Due to its low detection energy threshold and its long operation, PAMELA was able to accurately measure the fluxes of several cosmic-ray species over a large energy range and study their time variations below a few tens of GeVs. In this presentation we will review PAMELA results on the time-dependent proton, helium and electron fluxes measured between a few tens of MeV/n and few tens of GeV/n from 2006 to 2014. Moreover, preliminary results of yearly energy spectra of deuterons, helium-3 and helium-4 nuclei below 1 GeV/n will be discussed. These measurements covered a time including the minimum phase of the 23rd solar cycle and the 24th solar maximum including the polarity reversal of the solar magnetic field. The PAMELA measurements have allowed to significantly improve the understanding of the charged-particle propagation through the Heliosphere, the charge-sign effect due to the drift motions of these particles and to calibrate state-of-the-art models of cosmic-ray transport in the Heliosphere.

27th European Cosmic Ray Symposium - ECRS
25-29 July 2022
Nijmegen, the Netherlands

*Speaker

PoS(ECRS)044

1. Cosmic-Ray solar modulation

Being electrically charged, Cosmic Rays (CRs) are affected by the ambient magnetic fields during their propagation in space. Crossing the boundaries of the Heliosphere, CRs interact with the turbulent supersonic solar wind (SW) ejected by the Sun and the heliospheric magnetic field (HMF), i.e. the solar magnetic field frozen in the SW. This interaction deflects, scatters and hampers the CR propagation through the Heliosphere in a complex way, which can be studied by analysing the fluxes measured by CR experiments.

Two main effects can be recognized in the CR energy spectrum measured at Earth: a decrease of the intensity at low energies, below a few tens of GeV, with respect to the Local Interstellar Spectrum (LIS), i.e. the CR energy spectrum outside the Heliosphere, and a time dependence of the intensity at low energies as a function of the solar activity. In particular, an anticorrelation was observed between the measured CR intensity and the solar activity, which varies its intensity from a minimum to a maximum value according to an 11-year solar cycle. This means a cyclic 11-year solar modulation with higher CR fluxes measured during the solar minimum phase, when the HMF is characterized by lower values and a more ordered field line structure, and lower CR fluxes during the solar maximum phase, when the Sun reverses its magnetic polarity and the HMF field line structure becomes chaotic [1]. Additionally, comparing the CR energy spectrum profile during two consecutive solar minimum phases, a sharper trend is observed during the period of negative polarity and a flatter shape during the period of positive polarity. This pattern is observed reversed when analysing particles of opposite charge. This points to a CR propagation affected by the drift motion determined by the HMF polarity and the particle charge sign. This entails that the CR solar modulation also depends on the 22-year cycle followed by the solar magnetic field strength and polarity [1].

All these effects found a formulation in the Parker's transport equation [2] including four major modulation mechanisms: convection, particle drift due to gradients, curvatures and the wavy current sheet of the HMF, diffusion described by a 3D diffusion tensor and adiabatic energy losses. This transport equation can not be solved exactly with analytical approaches, but several models have been developed to solve it numerically and reproduce the experimental data.

2. The PAMELA experiment

PAMELA (Payload for Antimatter Matter Exploration and Light-nuclei Astrophysics) was an Earth-orbiting experiment designed to detect CRs, with a particular focus on the antiparticle component [3]. PAMELA was installed on board the Russian Resurs-DK1 satellite inside a pressurized container and launched into orbit on the 15th June 2006. From that moment, PAMELA took data almost continuously until the 23rd January 2016.

PAMELA was composed of the following detectors: a Time-of-Flight system, a magnetic spectrometer, an anticoincidence system, an electromagnetic calorimeter, a shower tail catcher scintillator and a neutron detector. Their combined use has allowed the measurements of the energy spectra and the composition of CRs over a wide energy range. For more details on the PAMELA apparatus see [4].

Figure 1

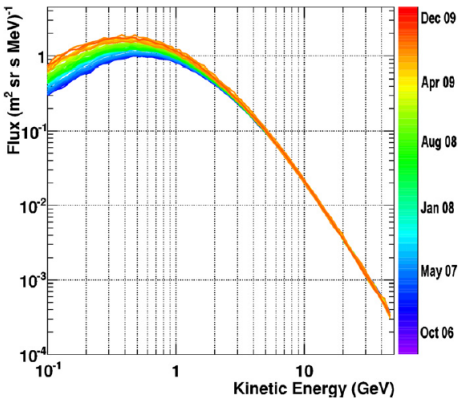

(a) Time evolution of the proton energy spectrum approaching the minimum of the 23rd solar cycle, from July 2006 (violet) to December 2009 (red) [5].

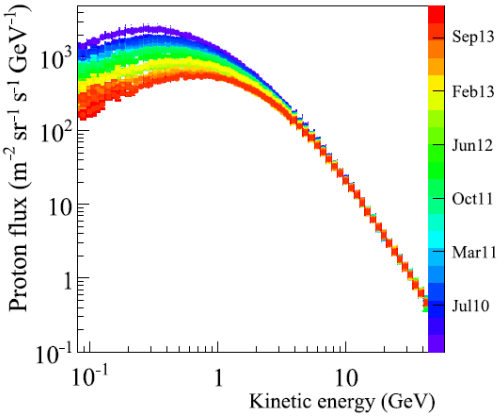

(b) Time evolution of the proton energy spectrum approaching the maximum activity of the 24th solar cycle, from January 2010 (blue) to February 2014 (red) [6].

3. The PAMELA studies of solar modulation

Due to its low detection energy threshold and its long operation PAMELA has been a key-experiment for studies of CR solar modulation. PAMELA semipolar orbit around Earth allowed the measurement of low-energy CRs at latitudes where the Störmer geomagnetic cut-off tends to zero. Its operation lasted for about ten years allowing to collect CR data during an almost whole solar cycle. In particular, PAMELA measured the CR energy spectra during the solar minimum phase of the anomalous long 23rd solar cycle and the solar maximum phase of the subsequent 24th solar cycle with a reversal of solar magnetic polarity in 2013. This kind of measurements are essential to improve the understanding and the modeling of the CR solar modulation. Energy spectra and their time evolution measured by the PAMELA experiment for the main CR species are reported hereinafter.

3.1 Time evolution of the proton energy spectra

The proton energy spectra were measured by PAMELA and reported from July 2006 to December 2009 in [5] and from January 2010 to February 2014 in [6]. The large statistics allowed the time variation to be followed on a Carrington-rotation time basis down to 400 MeV. The time evolution of the Carrington-rotation proton energy spectra are shown for the solar minimum period in Figure 1a and for the solar maximum period in Figure 1b. The energy dependence of the solar modulation is clearly evident, the low-energy protons are most affected with an increase at 100 MeV of a factor of about 2.75 from July 2006 to December 2009 reaching the solar minimum and then a decrease of a factor of about 10 approaching the solar maximum in February 2014. Above 30 GeV the flux does not present any temporal variation within the experimental uncertainties. The spectral shape is also observed to slightly change, becoming progressively softer during the solar minimum phase as more low-energy cosmic rays could reach the inner Heliosphere, with the spectral peak shifting towards lower kinetic energy values from 410 MeV/n in 2006 to 270 MeV/n in 2009. It becomes progressively harder during the solar maximum phase with the spectral peak shifting back

Figure 2

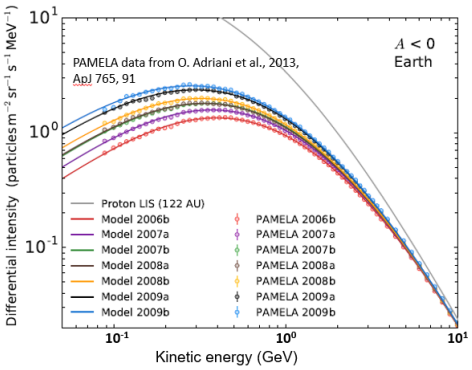

(a) Proton energy spectra (coloured circles) overlaid by modeled spectra (coloured solid lines) computed from the LIS at 122 AU (grey lines) [7].

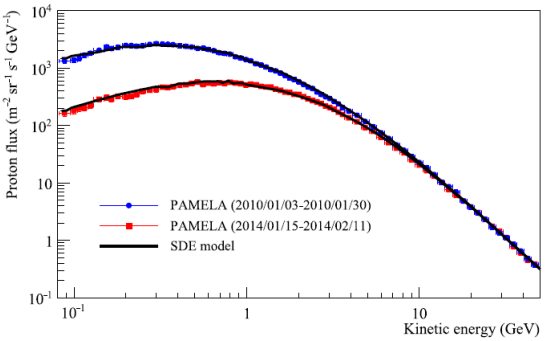

(b) Proton energy spectra measured in two Carrington rotations during 2010 (blue circles) and 2014 (red squares) overlaid by modeled spectra (black curves) [6].

to higher kinetic energies up to 700 MeV in 2014.

The Carrington-rotation proton energy spectra measured during the solar minimum period were averaged to obtain seven six-month proton spectra from July 2006 to December 2009 shown in Figure 2a, where they are overlaid by the corresponding spectral curves computed by a 3D numerical model of CR propagation in the Heliosphere [7]. Such a comparison was performed also for two Carrington-rotation proton energy spectra measured during the solar maximum, as shown in Figure 2b, when the solar modulation modeling is particularly challenging due to the complex HMF pattern. The model solves numerically the Parker's transport equation using as input the LIS as well as data about the HMF intensity and polarity, the heliospheric-current-sheet tilt angle and the SW velocity. The propagation parameters are tuned through a comparison of the computed spectra with the observed ones. A full discussion of the whole procedure can be found in [1] [8]. Both for solar minimum and maximum phases, the model reproduces the features of the energy spectra over the wide energy range, in particular, the intensity values where the spectra peak and how the peak shifts to higher energies while the spectrum decreases with increased modulation. This kind of comparisons is essential to optimize the shape of the LIS and the values of the propagation parameters for different heliospheric conditions.

Currently, an analysis of isotopic separation for the CR hydrogen detected by PAMELA is also underway and yearly proton and deuteron differential low-rigidity spectra and their time evolution from 2006 to 2014 will be the topic of a future publication. Details about this analysis are reported in [9].

3.2 Time evolution of the helium energy spectra

The helium energy spectra were measured by PAMELA down to 100 MeV/n from July 2006 to December 2009 [10] and from January 2010 to September 2014 [11]. Until 2009 the time variation was analysed on a Carrington-rotation time basis with the only exception of the last four Carrington-rotation energy spectra merged into a single one for statistical reasons. From January 2010 the helium fluxes were evaluated on a three Carrington-rotation time basis due to the decrease of the statistics caused by random failures of a few front-end chips in the PAMELA tracking system

Figure 3

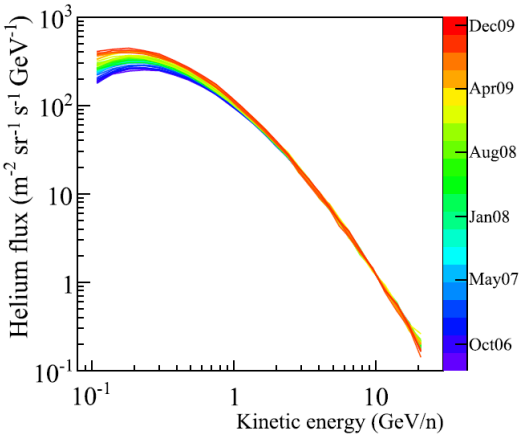

(a) Time evolution of the helium energy spectrum approaching the minimum of the 23rd solar cycle, from July 2006 (violet) to December 2009 (red) [10].

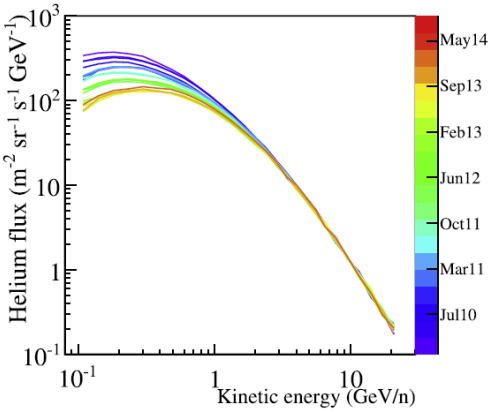

(b) Time evolution of the helium energy spectrum from the minimum to the maximum activity of the 24th solar cycle, from January 2010 (violet) to September 2014 (red) [11].

particularly significant from the end of 2009 forward. The time evolution of the helium energy spectra are shown for the solar minimum period in Figure 3a and for the solar maximum period in Figure 3b. As expected, the low-energy range is the most affected by the solar modulation: the fluxes measured at about 100 MeV/n increase by a factor of two from middle 2006 to the end of 2009 when the solar minimum was reached and they decrease by a factor of about four from January 2010 to September 2014 approaching the solar maximum. This modulation effect gets gradually smaller moving towards higher kinetic energies to become negligible with respect to the experimental uncertainties at kinetic energies above 15 GeV/n. The spectral shape was also observed to vary, it becomes progressively softer during the solar minimum phase with the spectral peak shifting from about 250 MeV/n in 2006 to about 150 MeV/n by the end of 2009, then it becomes gradually harder during the solar maximum phase with the spectral peak moving back to 300 MeV/n in September 2014.

The solar modulation of the helium fluxes was compared to that observed in the proton fluxes for the same period calculating the proton-to-helium flux ratios for five rigidity ranges as a function of time as in Figure 4. For the ratio calculation, the last four proton Carrington-rotation energy spectra in 2009 were averaged for consistency with the helium time basis, while after 2009 a weighted average over nine Carrington rotations was performed on both protons and helium to reduce the statistical fluctuation for those data. Data from late 2009 to early 2010 are missing due to a period of shut down of the satellite housing the PAMELA instrument for technical maintenance. For each rigidity interval the data were fitted with a constant function before and after the 2010 interruption, the fitted lines are plotted in Figure 4. It can be noticed that the proton-to-helium ratios have an opposite time dependence in the lower and higher rigidity ranges: in the lower rigidity intervals the ratios decrease from the solar minimum to the solar maximum phase, whereas in the higher rigidity intervals the ratios tend to increase from the solar minimum to the solar maximum phase. These trends were also studied comparing the observed ratios with those obtained by the AMS-02 experiment from 2 GV [12] and with the modeled curves computed with the Force-Field approximation [13], a simplified

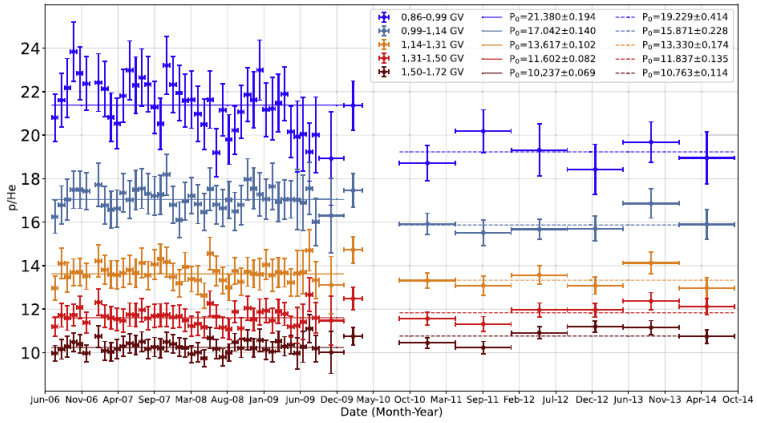

Figure 4: Time profiles of the proton-to-helium flux ratios for the five rigidity intervals specified in the legend. The error bars are the quadratic sum of statistical and systematic errors. The lines and P_0 parameters resulting from the fit with a constant in each rigidity bin in the solar minimum (solid lines) and maximum (dashed lines) periods are also shown [11].

analytical solution of the Parker's transport equation. A good agreement with both the AMS-02 data and Force-Field predictions was obtained [11].

Currently, an analysis of isotopic separation for the CR helium nuclei detected by PAMELA is underway, details in [14].

3.3 Time evolution of the electron and positron energy spectra

Galactic electrons and positrons are important CR components. Being leptons, both electrons and positrons undergo different energy-loss processes in Galactic space with respect to the CR nuclear component at the same kinetic energy, so that they can provide information otherwise not accessible from the study of the other CR species.

Electron and positron energy spectra were measured between 80 MeV and 50 GeV by PAMELA and reported for the solar minimum phase on a six-month time basis in [15] and [16] respectively. The seven six-month electron and positron energy spectra from July 2006 to December 2009 are shown in Figure 5a and Figure 5b respectively. The low-energy fluxes are the most affected by the solar modulation, moving from 2006 to late 2009 electron fluxes show an increase by a factor of 3.5 at 100 MeV, whereas positron fluxes increase by a factor of 6 at around 200 MeV. These increases are observed to be gradually reduced moving to higher energies to become negligible above 30 GeV with respect to the experimental uncertainties. The observed spectral shapes are also modulated by the varying solar activity, electron energy spectra exhibit a peak between 500 - 800 MeV shifting gradually to lower kinetic energies during the solar minimum period; analogously positron energy spectra exhibit a characteristic peak just below 1 GeV which gradually shifts to lower values approaching the solar minimum. At lower energy values, electron and positron spectra decrease and reach minimum values around 80-200 MeV. These spectra minima shift gradually to higher energies with the decreasing solar activity, making the spectral shapes progressively softer. Below 80 MeV, electron and positron spectra turn up as the diffusion mechanisms become dominant in contrast to protons, helium and other CR nuclei for which adiabatic energy losses dominate.

Figure 5

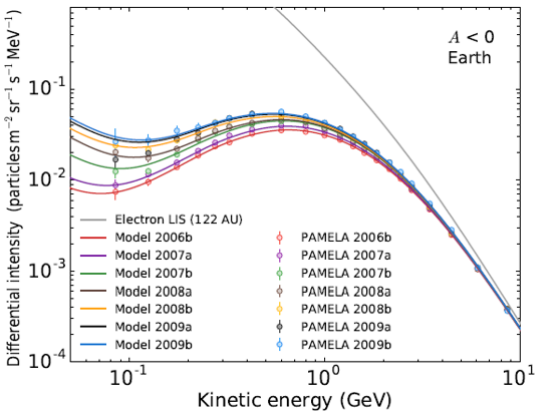

(a) Electron energy spectra for seven six-month–averaged periods from July 2006 to December 2009 (colored circles) overlaid by modeled spectra (coloured solid lines) computed from the LIS at 122 AU (grey line) [7].

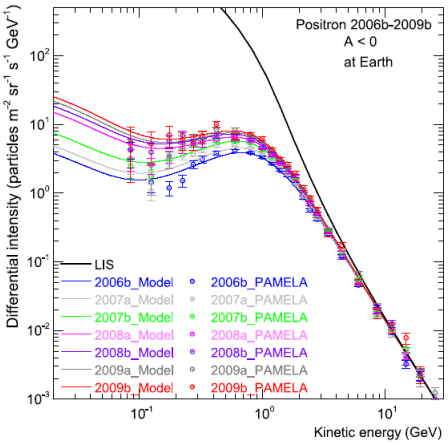

(b) Positron energy spectra for seven six-month–averaged periods from July 2006 to December 2009 (colored circles) overlaid by modeled spectra (coloured solid lines) computed from the LIS at 122 AU (black line) [17].

In Figure 5a and Figure 5b the measured energy spectra are overlaid by the modeled spectra computed with a 3D numerical model starting from the input LIS (black curves) at the Heliosphere outer boundary and accounting for the charge-sign effect induced by the drift motions. The modeled spectral curves reproduce well the time evolution and the main spectral features of the observed electron and positron energy spectra. The agreement worsens only with the measured positron fluxes below 200 MeV, which are however affected by significant systematic uncertainties [16][17]. The positron-to-electron flux ratio measured by the PAMELA experiment [18] is shown in Figure 6 for the energy range 1.0 GeV - 2.5 GeV and for the period July 2006 - December 2015. The shaded region indicates the HMF reversal period during which the HMF polarity is not well defined. The ratio is observed to increase by about 20% up to the end of 2009, then it starts to decrease continuously up to the middle 2012 as the solar activity increases, it remains almost the same for most of 2013, followed by a slow increase up to the end of 2014 with a sudden rise and progressive increase during 2015. The ratio ends up by being a factor of 1.5 larger than in 2006 as an effect of the change of drift motion pattern with the reversal of the HMF polarity. In Figure 6 the positron-to-electron flux ratios are overlaid by the corresponding ratios computed by the 3D numerical model of CR solar modulation as well. The model used exactly the same propagation parameters for the two types of leptons [19]. The computed ratios follow the same trend than the observed ratios allowing to evaluate the relevance of the different solar modulation mechanisms as a function of solar activity and the HMF polarity. It was found that though drifts played an important role in modulating these CRs from the 2006 to 2009, the period was diffusion dominated. For more details see [19] [20].

4. Conclusions

We reviewed the main results obtained by the PAMELA collaboration for the major CR species at the low energies, which are the most affected by solar modulation, for almost a whole solar

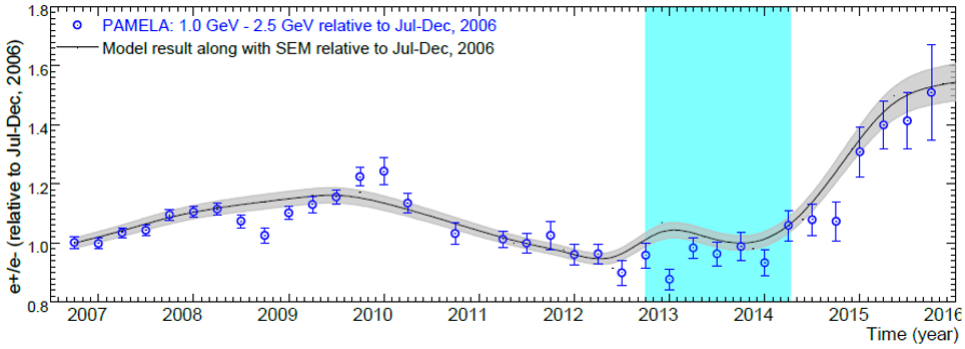

Figure 6: Measured e^+/e^- ratio in the kinetic energy interval 1.0 GeV - 2.5 GeV (blue circles [18]) averaged over 3-months for the period July 2006 - December 2015, overlaid by the computed e^+/e^- (solid line with a standard error of mean). Both ratios are normalized with respect to July - December 2006. The shaded region indicates the period without a well-defined HMF polarity [19].

cycle from the middle of 2006 to the end of 2015, with a reversal of HMF polarity in 2013. The comparison of the measured energy spectra with the predictions computed by a 3D numerical model of CR solar modulation allows to progressively improve the understanding and the modeling of the mechanisms ruling the CR propagation in the Heliosphere for different solar-modulation conditions. This study performed for the main CR species is going to be extended also for the major CR isotopes detected by PAMELA.

References

[1] M. S. Potgieter, Living Rev. Solar Phys. 10 (2013) 3.

[2] E. N. Parker P&SS 13 (1965) 9.

[3] O. Adriani et al., Phys. Rep. 544 (2014) 323-370.

[4] P. Picozza et al., Astropart. Phys. 27 (2007) 296-315.

[5] O. Adriani et al., ApJ 765 (2013) 91.

[6] M. Martucci et al., ApJL 854 (2018) L2.

[7] M. S. Potgieter and E. E. Vos A&A 601 (2017), A23.

[8] M. S. Potgieter, PhD thesis, Potchefstroom University, South Africa, 1984.

[9] A. Lenni, PhD thesis, University of Trieste, Italy, 2022.

[10] N. Marcelli et al., ApJ 893 (2020) 145.

[11] N. Marcelli et al., ApJL 925 (2022) L24.

[12] M. Aguilar et al., PhRvL 121 (2018), 051101.

[13] L. J. Gleeson and W. I. Axford, ApJ 154 (1968), 1011.

[14] A. Lenni et al., PoS ICRC 2021, 1310.

[15] O. Adriani et al., ApJ 810 (2015), 142.

[16] R. Munini, PhD thesis, University of Trieste, Italy, 2013.

[17] O. P. M. Aslam et al., ApJ 873 (2019), 70.

[18] O. Adriani et al., PhRvL 116 (2016), 241105.

[19] O. P. M. Aslam et al., ApJ 909 (2021), 215.

[20] M. S. Potgieter, Adv. Space Res. 60 (2017), 848-864.

Full Author List: PAMELA Collaboration

O. Adriani[1,2], G. C. Barbarino[3,4], G. A. Bazilevskaya[5], R. Bellotti[6,7], M. Boezio[8,9], E. A. Bogomolov[10], M. Bongi[1,2], V. Bonvicini[8], A. Bruno[6], F. Cafagna[7], D. Campana[2], P. Carlson[11], M. Casolino[12,13], G. Castellini[14], C. De Santis[12], A. M. Galper[16], S. V. Koldashov[16], S. Koldobskiy[16], A. N. Kvashnin[10], A. Lenni[8,9,17], A.A. Leonov[16], V.V. Malakhov[16], L. Marcelli[12], N. Marcelli[8,9], M. Martucci[18,19], A. G. Mayorov[16], W. Menn[20], M. Merge[12,18], V. V. Mikhailov[16], E. Mocchiutti[8], A. Monaco[6,7], N. Mori[2], R. Munini[8,9], G. Osteria[4], B. Panico[4], P. Papini[2], M. Pearce[11], P. Picozza[12,18], M. Ricci[19], S. B. Ricciarini[2,14], M. Simon[20], A. Sotgiu[12], R. Sparvoli[12,18], P. Spillantini[16,21], Y. I. Stozhkov[5], A. Vacchi[8,22], E. Vannuccini[2], G.I. Vasilyev[10], S. A. Voronov[16], Y. T. Yurkin[16], G. Zampa[8] and N. Zampa[8]

[1] University of Florence, Department of Physics, I-50019 Sesto Fiorentino, Florence, Italy. [2] INFN, Sezione di Florence, I-50019 Sesto Fiorentino, Florence, Italy. [3] University of Naples "Federico II," Department of Physics, I-80126 Naples, Italy. [4] INFN, Sezione di Naples, I-80126 Naples, Italy. [5] Lebedev Physical Institute, RU-119991, Moscow, Russia. [6] University of Bari, Department of Physics, I-70126 Bari, Italy. [7] INFN, Sezione di Bari, I-70126 Bari, Italy. [8] INFN, Sezione di Trieste, I-34149 Trieste, Italy. [9] IFPU - Institute of Fundamental Physics of the Universe, I-34151 Trieste, Italy. [10] Ioffe Physical Technical Institute, RU-194021 St. Petersburg, Russia. [11] KTH, Department of Physics, and the Oskar Klein Centre for Cosmoparticle Physics, AlbaNova University Centre, SE-10691 Stockholm, Sweden. [12] INFN, Sezione di Rome "Tor Vergata," I-00133 Rome, Italy. [13] RIKEN, EUSO team Global Research Cluster, Wako-shi, Saitama, Japan. [14] IFAC, I-50019 Sesto Fiorentino, Florence, Italy. [15] Space Science Data Center—Agenzia Spaziale Italiana, via del Politecnico, s.n.c., I-00133, Roma, Italy. [16] MEPhI: National Research Nuclear University MEPhI, RU-115409, Moscow, Russia. [17] University of Trieste, Department of Physics, I-34127 Trieste, Italy. [18] University of Rome "Tor Vergata," Department of Physics, I-00133 Rome, Italy. [19] INFN, Laboratori Nazionali di Frascati, Via Enrico Fermi 40, I-00044 Frascati, Italy. [20] University of Siegen, Department of Physics, D-57068 Siegen, Germany. [21] Istituto Nazionale di Astrofisica, Fosso del cavaliere 100, I-00133 Roma, Italy. [22] University of Udine, Department of Mathematics, Computer Science and Physics Via delle Scienze, 206, Udine, Italy.